

ARTICLES

Perfluoro-Poly(ethers) with Hydroxyl End Groups: Analysis by TOF-SIMS

Paul H. Kasai*

IBM Research Division, Almaden Research Center, San Jose, California 95120

A. M. Spool*

IBM Storage Systems Division, San Jose, California 95193

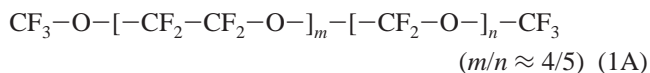
Received: February 20, 1998; In Final Form: June 9, 1998

TOF-SIMS spectra of perfluoro-poly(ethers) (PFPE) with hydroxyl end group(s), Fomblin Z-DOL, Krytox-OH, and Demnum-SA, were analyzed. Previously we have observed that while the positive-ion TOF-SIMS spectra of nonfunctionalized PFPEs are complex and compressed toward the low mass end, the negative-ion spectra show intense simple patterns persisting into a high mass region surpassing the mean molecular weight of the polymer. The rich negative-ion spectra of nonfunctionalized PFPEs are ascribed to anions generated by one-event dissociative capture of low-energy secondary electrons by ether oxygens of the polymer backbone: $R-O-R' + e^- \rightarrow R-O^- + \cdot R'$. In stark contrast to nonfunctionalized PFPEs, PFPEs with hydroxyl end group(s) showed, in the positive-ion spectra, a fragmentation pattern persisting into the high mass region and a pattern clearly associated with the parent molecule (molecular weight) distribution. In the negative-ion spectra, the pattern due to anions $R-O^-$ encompassing the hydroxyl sector was totally absent. The observed anomalies can be accounted for if one postulates that PFPEs with hydroxyl end group(s) have a strong propensity to ionize at the hydroxyl sector. A possible relevance of such a propensity to the bonding mechanism of Z-DOL (Fomblin Z with hydroxyl end groups) to the carbon overcoat of magnetic recording disks is conjectured.

Introduction

Perfluoro-poly(ethers) (PFPEs) are currently the lubricant of choice for magnetic recording disks.¹ They are also in use as lubricants in such severe environments as aerospace engines and satellite instruments.² Excellent lubricity aside, a wide liquid-phase temperature range, low vapor pressure, small temperature dependency of viscosity, high thermal stability, and low chemical reactivity are the attributes that have led to these high-performance applications. Commercially available and most-often discussed PFPEs are those known by the brand names Fomblin Z, Krytox, and Demnum. Their formulas are as follows.

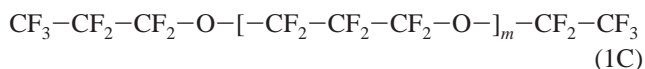
Fomblin Z:



Krytox:

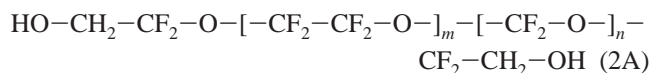


Demnum:

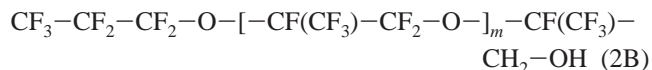


The PFPE most commonly used for disk lubrication is Fomblin Z with hydroxyl end groups (known by the brand name Z-DOL). It is bifunctional, i.e., the molecular chain is terminated by the hydroxyl substituent at both ends. Krytox and Demnum are also available with the hydroxyl end group. They are mono-functional, however. The formulas of commercially available PFPEs with hydroxyl end groups are as follows.

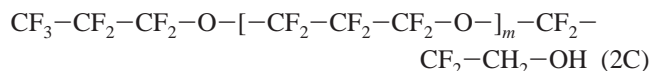
Fomblin Z-DOL:



Krytox-OH:



Demnum-SA:



PFPEs suitable for disk lubrication are of molecular weight 2000–5000 corresponding to 12–30 monomer units in each chain.

For sake of brevity, we shall use notations Z-S, K-S, and D-S to indicate the specific nonfunctionalized PFPEs, a notation

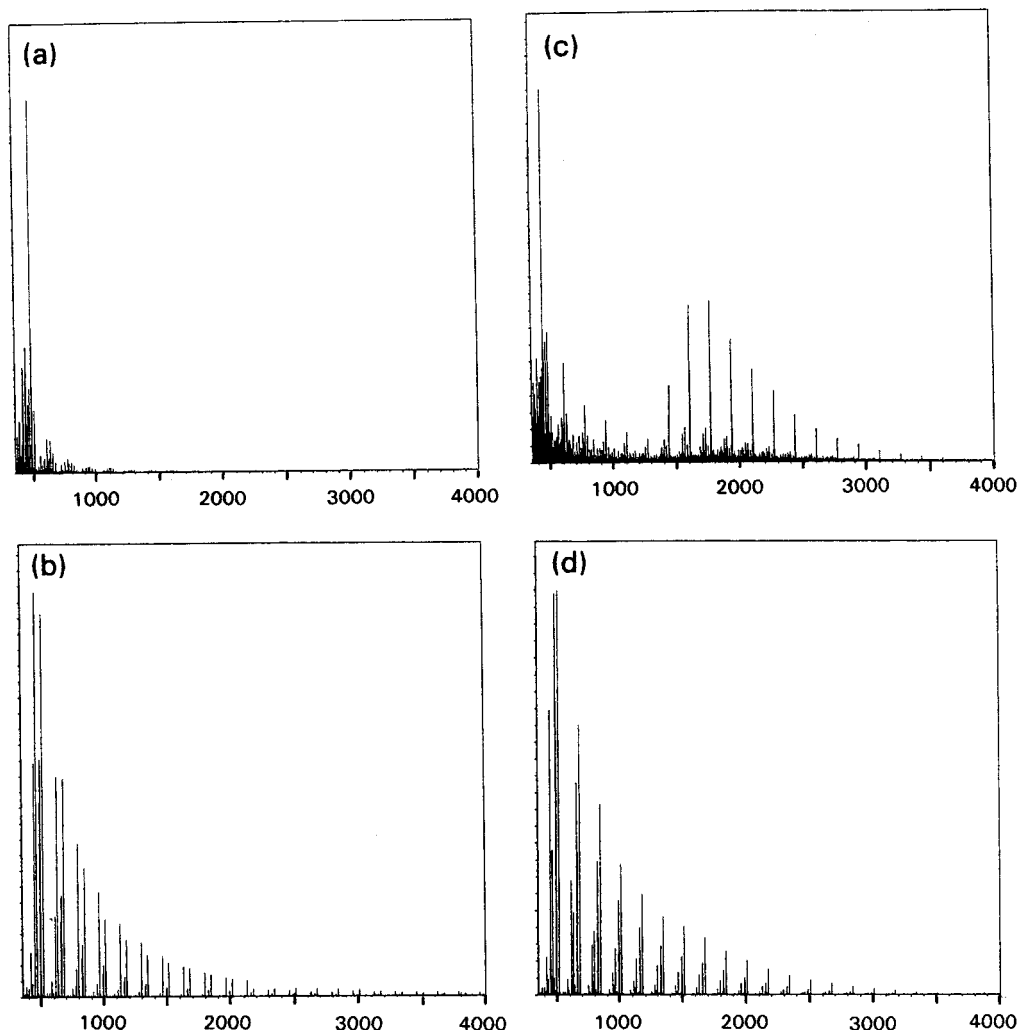
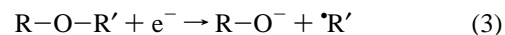


Figure 1. TOF-SIMS spectra observed from D-S and D-OH: (a) D-S (positive ions), (b) D-S (negative ions), (c) D-OH (positive ions), and (d) D-OH (negative ions). The number-averaged molecular weight (determined from F-19 NMR) of the particular D-OH was 2000.

such as PFPE-OH to indicate PFPEs generically with hydroxyl end group(s) and notations such as Z-OH, for example, to indicate the specific PFPE with hydroxyl end group(s).

Recently we reported on a TOF-SIMS study of nonfunctionalized PFPEs.³ We observed that while the positive-ion spectra of nonfunctionalized PFPEs are extremely complex and compressed toward the low-mass end, the negative-ion spectra have intense but simple repetitive patterns persisting into the high-mass region, surpassing the mean MW of the polymers. It is well-known that when a beam of high-energy X-rays, electrons, or positive ions traverses through fluid media (where little energy is required for desorption of molecules), essentially all of the energy dissipation (of the primary beam) occurs through ionization of media molecules and "chemical events" are caused by numerous secondary electrons generated through cascading processes.⁴ It is also well-known that large organic molecules, upon impact with high-energy electrons, undergo (multiple) fragmentation and generate series of positively charged fragments weighted toward the low-mass end.⁵ The positive-ion spectra of nonfunctionalized PFPEs were, hence, attributed to such fragments generated by energetic secondary electrons. It is surmised that such processes occur closer to the trajectory of the primary ion beam. We proposed and substantiated that the persistent negative-ion patterns are due to negative ions produced by a one-step dissociative capture of secondary electrons of thermal energy at ether oxygens of PFPEs.



It is surmised that the process occur in the region circumjacent to the area of primary ionization, where intact parent molecules are still around.

We report here the result of a TOF-SIMS study of commercially important PFPE-OH. In stark contrast to nonfunctionalized PFPEs, PFPE-OH showed, in the positive-ion spectrum, not only a fragmentation pattern extending into the mean MW of the polymers, but also a pattern clearly associated with the parent molecule distribution. An anomaly was also observed in the negative-ion spectrum; for D-OH, for example, the negative-ion pattern due to fragments R-O^- encompassing the hydroxyl end group was totally missing. It will be shown that these anomalies can be accounted for if one postulates that PFPE-OH has a strong propensity to become ionized at the hydroxyl sector.

Experimental Section

PFPEs examined in the present study, Fomblin Z, Krytox, and Demnum (both functionalized and nonfunctionalized forms), were obtained from Montefluos (of Italy), Du Pont (of USA), and Daikin Industries (of Japan), respectively.

TOF-SIMS spectra were obtained from samples smeared onto Si wafers. All the analyses described below may, hence, be construed as those of fluid bulk materials. The spectral

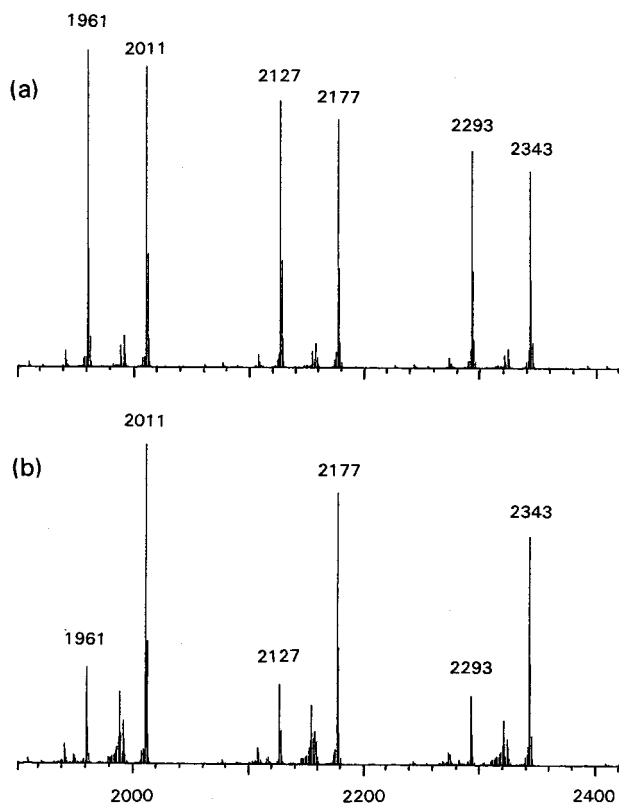


Figure 2. Negative-ion spectra of D-S and D-OH. Central sections of Figure 1b and d are shown in an expanded scale.

measurements were performed using a Charles Evans and Associates TRIFT spectrometer. This instrument has been described in detail elsewhere.^{6,7} The primary ions used for most of this work were from a pulsed Cs^+ source operating at 11 keV. Secondary-ion extraction was accomplished with a ± 3 keV bias on the sample. For all spectra obtained in this study, the total ion dose was kept below 10^{12} ions cm^{-2} , lower than the generally accepted static limit.⁸ All the spectra are shown in linear vertical scale, and the same vertical scale (the ion counts) may be assumed for each set of spectra shown in comparison.

TOF-SIMS Spectra and Analyses

D-S and D-OH. Figure 1a and b show, respectively, the positive- and negative-ion TOF-SIMS spectra (for the mass range 500–4000 amu) observed from D-S. The paucity of signals in the positive-ion spectrum is in strong contrast to the profusion of signals in the negative-ion spectrum. Most of the positive ions were detected in the mass range below 500 amu. As stated earlier, the negative-ion spectrum (Figure 1b) is characterized by a simple repetitive pattern extending across the range; here, in particular, the doublet of 50 amu separation is repeated with a 166 amu interval (see Figure 2a for a section of the negative-ion spectrum shown in an expanded scale). These

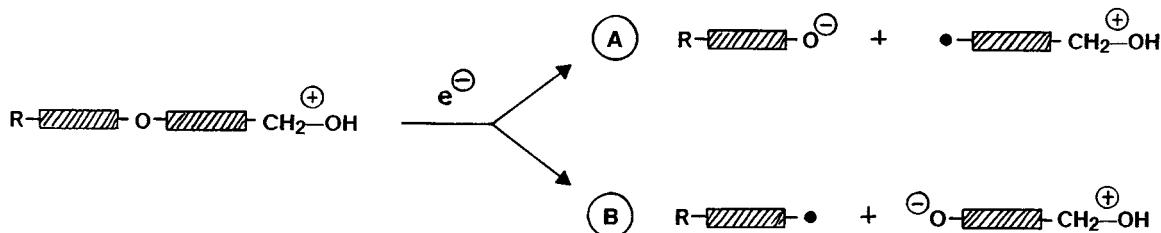
anions are ascribed to R-O^- resulting from the dissociative electron capture reaction 3 manifested on D-S. The 166 amu interval is due to the mass of the repeat unit, $-\text{CF}_2-\text{CF}_2-\text{CF}_2-\text{O}-$, and the 50 amu separation of the doublet is due to the mass difference of the perfluoropropoxy and perfluoroethoxy end groups at the opposite ends of the molecular chain (see formula 1C).

Figure 1c and d show, respectively, the positive- and negative-ion TOF-SIMS spectra (the same mass range) observed from D-OH. The number-averaged molecular weight of this particular D-OH (determined from its F-19 NMR spectrum) is ~ 2000 . It is most intriguing that in stark contrast to D-S, the positive-ion spectrum of D-OH shows not only a fragmentation pattern of significant intensity, but also a pattern clearly associated with the parent molecule distribution. Figure 2a and b show, in an expanded scale, central sections of the negative-ion spectra of D-S and D-OH. It can be readily recognized that in the negative-ion spectrum of D-OH, the pattern due to anions R-O^- encompassing the hydroxyl end group is totally absent. It should appear shifted downward by 38 amu from that of R-O^- encompassing the propoxy end group (see formula 2C).

Thus, there are three anomalies in the TOF-SIMS spectra of D-OH: (1) the missing negative-ion pattern due to R-O^- encompassing the hydroxyl end group, (2) a positive-ion fragmentation pattern, and (3) a positive-ion pattern related to the parent molecule distribution. An examination by a semiempirical molecular orbital method (AM1)⁹ of short PFPEs revealed that the attachment of the hydroxyl end group, $-\text{CF}_2-\text{CH}_2-\text{OH}$, creates the highest occupied molecular orbital (HOMO) at ~ 2 eV above all other occupied orbitals of the system. The HOMO is completely localized in the hydroxyl sector. We, hence, postulate that during the TOF-SIMS experiment, many of the PFPE-OH molecules in the region circumscribed to the area of primary ionization become ionized on impact with secondary electrons, the energy of which is not sufficient to ionize nonfunctionalized PFPE but sufficient to ionize PFPE-OH at the hydroxyl sector. When these molecular cations capture an electron of yet lower energy and undergo the dissociative process, the two different paths in Scheme 1 are plausible. The molecular cations initially formed would account for the positive-ion pattern of the parent molecule distribution. The dissociation path A would account for both the negative-ion fragmentation pattern of R-O^- encompassing the propoxy end group and the anomalous positive-ion fragmentation pattern. The dissociation path B would offer an explanation for a lesser presence of negative-ion signals due to R-O^- encompassing the hydroxyl end group. The total absence of this type of anions revealed in the negative-ion spectrum (Figure 2) is surprising. It may be that such anions have an even stronger propensity to ionize at the hydroxyl sector, thus averting detection.

Figure 3 shows, in an expanded scale, a central section of the positive-ion spectrum observed from D-OH (Figure 1c); the peaks belonging to the tail end of the fragmentation pattern and

SCHEME 1



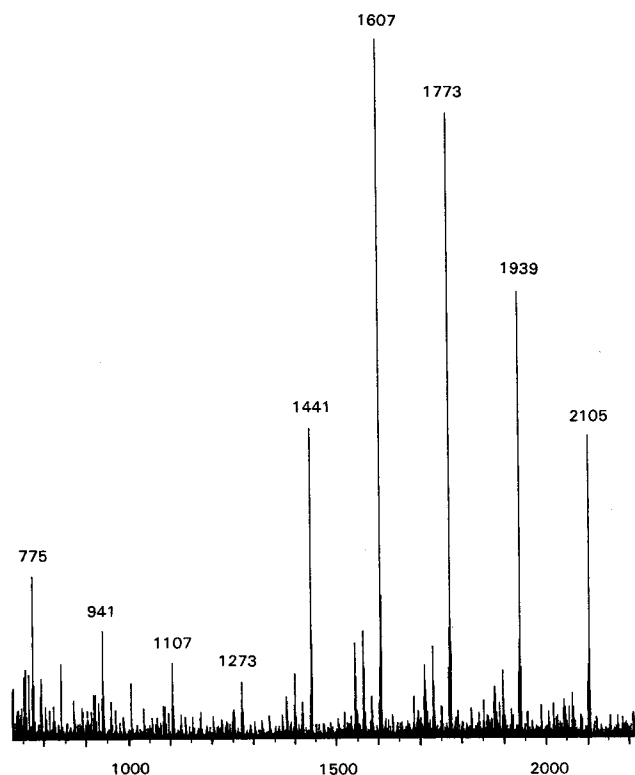
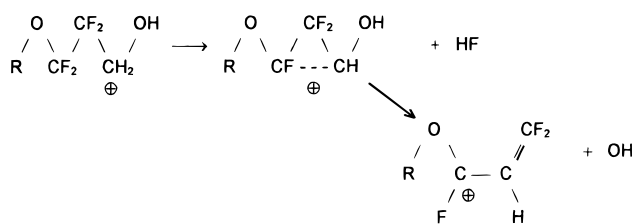
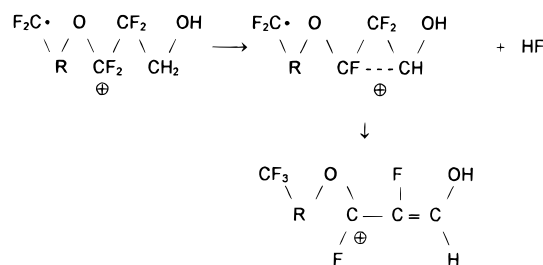


Figure 3. Positive-ion spectrum of D-OH. The section encompassing the tail end of the fragmentation pattern and the lower mass end of the molecular pattern is shown in an expanded scale.

the peaks belonging to the lower mass end of the molecular weight distribution are seen and identified with the respective amu values. It can be readily shown that the mass numbers of the *observed parent molecular cations* are downshifted by 37 amu from those of the corresponding intact molecules. The combined loss of HF and OH units would account for the difference. The mass numbers of the observed positive-ion fragments are downshifted by 20 amu from those expected from reaction path A. The loss of HF would account for the difference. We believe that in the case of D-OH, the following dissociation and/or intramolecular abstraction occur involving the ionized hydroxyl sector (in order to achieve the more stable allylic form of the cation). For the molecular cations:



For the positive-ion fragments:



K-S and K-OH. The overall characteristics of the TOF-SIMS spectra observed from K-S and K-OH were essentially

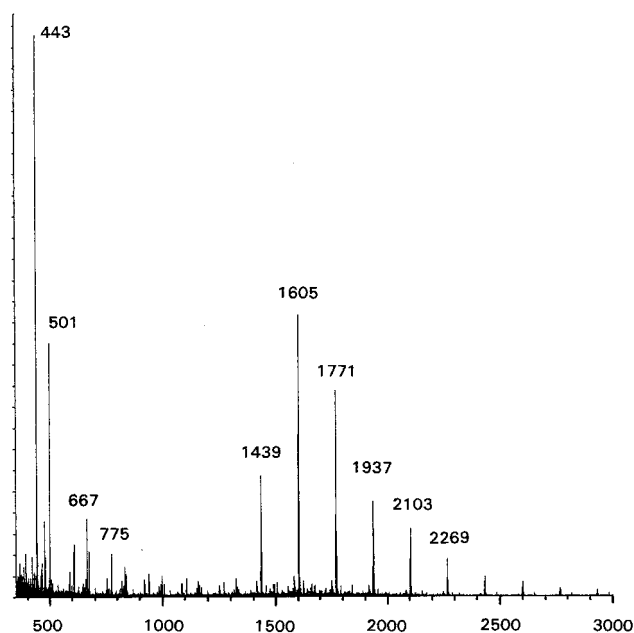
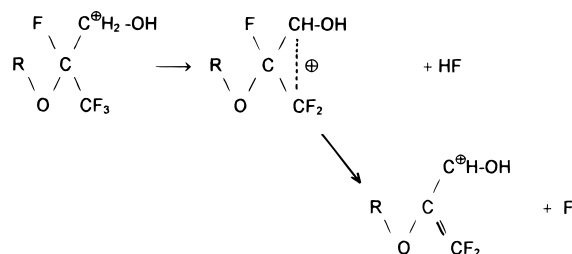


Figure 4. Positive-ion spectrum observed from K-OH. The number-averaged molecular weight (determined from F-19 NMR) of this particular K-OH was 1500.

identical to those observed from D-S and D-OH (cf. Figure 1a–d). The TOF-SIMS spectra of K-OH thus revealed the same three anomalies observed from D-OH, the missing negative-ion pattern due to R-O^- encompassing the hydroxyl end group, a positive-ion fragmentation pattern (though not as intense as that seen from D-OH), and a positive-ion pattern related to the parent molecule distribution. Figure 4 shows the positive-ion spectrum observed from a particular lot of K-OH. Its number-averaged molecular weight had been determined by F-19 NMR as 1500. The mass numbers of several prominent peaks belonging to the parent molecule distribution pattern are given. They are consistently 39 amu downshifted from those expected for the intact parent molecules. The difference is attributed to the loss of HF and F at the ionized hydroxyl sector.



Z-S and Z-OH. Figure 5a and b show, respectively, the positive- and negative-ion TOF-SIMS spectra observed from Z-S. Again, the paucity of signals in the positive-ion spectrum is in strong contrast to the profusion of signals in the negative-ion spectrum. The complexity of the negative-ion pattern is due to the random permutation of the ethylene oxide and methylene oxide units in the linear linkage of Fomblin Z polymer (see formula 1A). Figure 5c and d show, respectively, the positive- and negative-ion TOF-SIMS spectra (the same mass ranges) observed from Z-OH. The number-averaged molecular weight of this particular Z-OH (determined from its F-19 NMR spectrum) is ~ 2000 . The presence of a positive-ion pattern related to the parent molecule distribution is clearly seen. It is thus strongly indicated that under the TOF-SIMS experimental condition, many of the Z-OH molecular chains

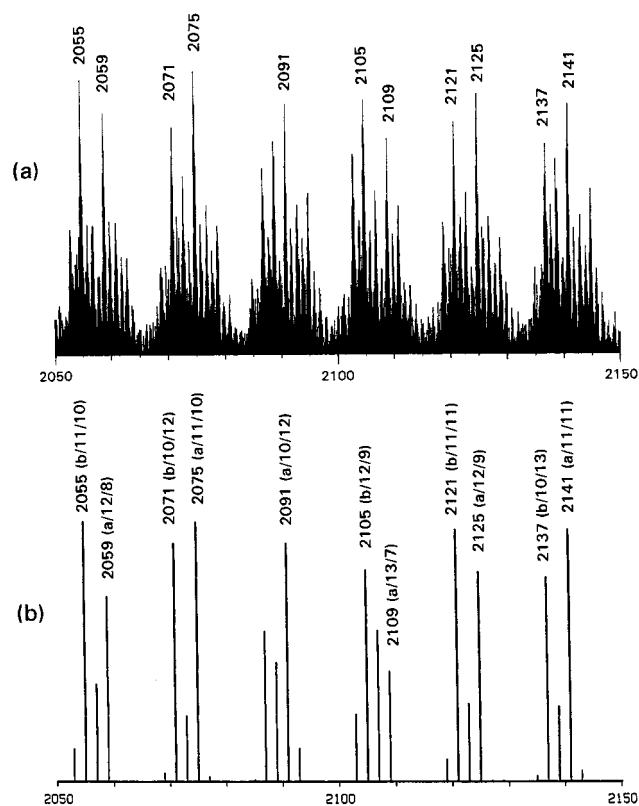


Figure 6. (a) Central section of the molecular weight pattern observed in the positive-ion spectrum of Z-OH (Figure 5c). The prominent peaks are identified with their mass numbers. (b) Computed pattern based on random permutation of $-\text{CF}_2-\text{CF}_2-\text{O}-$ and $-\text{CF}_2-\text{O}-$ units. Major peaks are identified with their mass numbers and notations such as $a/m/n$ indicating that the peak belongs to type a and contains m and n units of $-\text{CF}_2-\text{CF}_2-\text{O}-$ and $-\text{CF}_2-\text{O}-$, respectively. See text for detail.

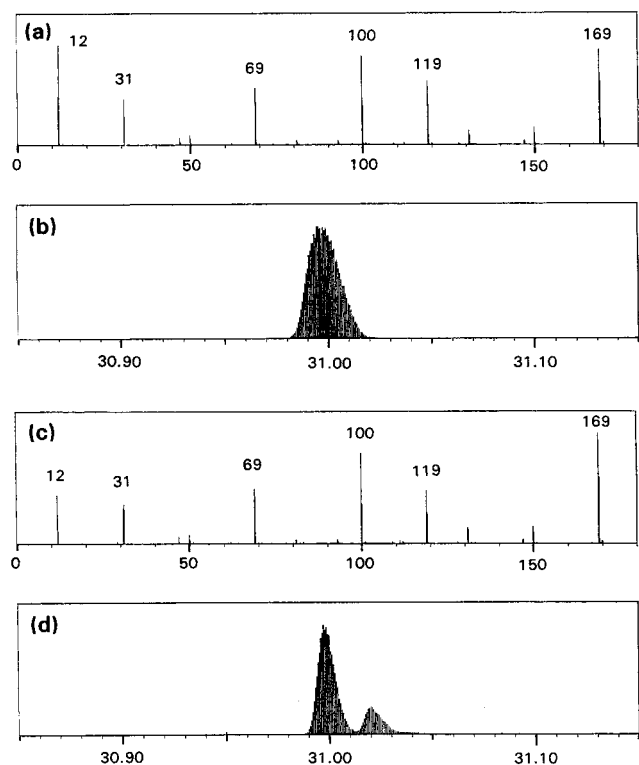


Figure 7. (a) Positive-ion spectrum of D-S (0–180 amu). (b) The 31 amu peak of the spectrum (a) examined in an expanded scale. (c) Positive-ion spectrum of D-OH (0–180 amu). (d) The 31 amu peak of the spectrum in c examined in an expanded scale.

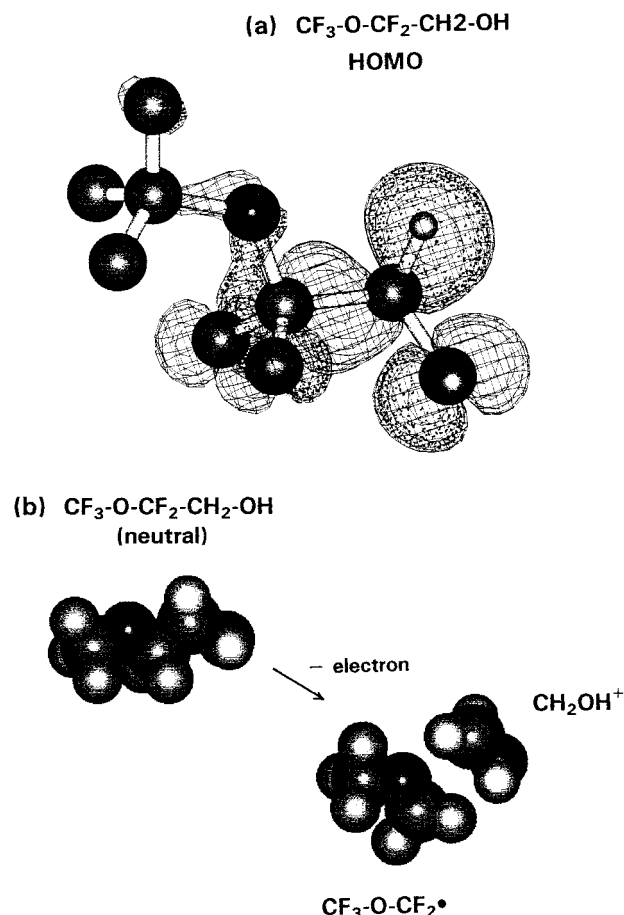


Figure 8. (a) Highest occupied molecular orbital (HOMO) of $\text{CF}_3-\text{O}-\text{CF}_2-\text{CH}_2-\text{OH}$ given by a semiempirical molecular orbital method (AM1). (b) The same theory also predicted that the molecule, if ionized, would spontaneously dissociate to yield the hydroxymethyl cation, CH_2OH^+ .

Detachment of CH_2OH Cation from Ionized PFPE-OH.

As stated earlier, examination of short PFPE and PFPE-OH by a semiempirical molecular orbital method (AM1)⁹ revealed that PFPE-OH should have a propensity to ionize at the hydroxyl sector. The theoretical study also revealed that molecules such as $\text{CF}_3-\text{CH}_2-\text{OH}$ or $\text{CF}_3-\text{O}-\text{CF}_2-\text{CH}_2-\text{OH}$, if ionized, would spontaneously dissociate to yield the hydroxymethyl cation (see Figure 8) $[\text{R}-\text{CF}_2-\text{CH}_2-\text{OH}]^+ \rightarrow \text{R}-\text{CF}_2^\bullet + \text{C}^+\text{H}_2-\text{OH}$. The corresponding detachment reaction was not predicted for the ionized $\text{CH}_3-\text{CH}_2-\text{OH}$ or $\text{CF}_3-\text{O}-\text{CH}_2-\text{CH}_2-\text{OH}$. Figure 7a shows the low-mass range (0–200 amu) of the positive-ion spectrum observed from D-S. Figure 7b shows, in an expanded scale, its peak at 31 amu due to CF^+ ions (mass number = 30.998). Figure 7c and d show the corresponding spectra observed from D-OH. The mass number of CH_2-OH is 31.018. The satellite peak 0.020 amu above the CF peak is, hence, assigned to CH_2-OH ions. The signals due to CH_2-OH ions were similarly observed in the positive-ion spectra of K-OH and Z-OH. The ionized hydroxyl sector of PFPE-OH, thus, undergoes either the CH_2OH^+ detachment process or the HF elimination elaborated earlier. On the basis of the total ion counts, it was estimated that the two processes occur at about equal probability.

Discussion

Conjecture on the Bonding Mechanism of Z-DOL to Carbon Overcoat. The present TOF-SIMS study of PFPE-

OH, thus, has revealed that the attachment of a hydroxyl end group to a PFPE chain imparts to the molecule a propensity to ionize. The highest occupied molecular orbital (HOMO) of $\text{CF}_3\text{—O—CF}_2\text{—CH}_2\text{—OH}$ given by the AM1 method is shown in Figure 8. It illustrates well how localized the *ionized state* would be in the hydroxyl sector of ionized PFPE-OH.

The magnetic (information) layer of magnetic storage disks are typically coated with a protective layer of sputtered carbon overcoat (COC). A PFPE lubricant layer (of a monomolecular thickness) is applied over COC for protection of the system from the tribological damage during operation. The mechanical and chemical stability of the PFPE/COC system is understandably a critical factor for the durability of the system. Yanagisawa measured heats of adsorption of Fomblin Z with a variety of end groups upon carbon powders of varying degrees of hybridization (sp^3 diamond to sp^2 graphite).¹⁰ He demonstrated that Fomblin Z with hydroxyl end groups, Z-DOL, has a singularly large (an order of magnitude larger) heat of adsorption compared to Fomblin Z of other end groups. He also showed the presence of a linear relation between the heat of adsorption of Z-DOL and the unpaired electron density of the carbon (as determined by ESR). No correlation was obtained between the heat of adsorption and the chemical functionality of the carbon surface (e.g., the density of the carboxylic group as determined by XPS). The ESR signal of an amorphous carbon decreased by 50% upon coating with Z-DOL lubricant. He then postulated that Z-DOL bonds to COC via interaction with dangling bonds (the unpaired electron) at the surface.

A radical center exposed at the surface should react immediately with atmospheric oxygen. Hoinks et al. independently examined the ESR signal (of the dangling bonds) of sputtered thin-film carbon.¹¹ They reported that the signal was not chemically affected by the presence of oxygen but showed a reversible line broadening when exposed to oxygen at high pressure (2 atm). The radical centers in carbons must be located

internally, and the porosity of the material must be such that atmospheric oxygen under high pressure can approach the centers close enough to broaden the signal but not enough to react permanently. It is well-known that localized radical centers constitute strong electron-acceptor centers. It has been estimated that alkyl radical centers have an electron affinity of ~ 25 kcal/mol.¹² It is enticing to conjecture that the bonding of PFPE-OH to COC might be ascribed to a charge-transfer process between electron-donating PFPE-OHs and electron-accepting dangling bonds. Direct contact between the hydroxyl sector and the unpaired electron site would not be required. Typically $\sim 5 \times 10^{20}$ unpaired electron centers are formed in 1 cm^3 of sputtered carbon.¹¹ Thus, for a carbon overcoat layer of 100 \AA thick, there would be one unpaired electron per 20 \AA^2 surface area, a quantify certainly sufficient to ensure monolayer coverage of the surface by Z-OH.

References and Notes

- (1) Moulder, J. F.; Hammond, J. S.; Smith, K. L. *Appl. Surf. Sci.* **1986**, 25, 446.
- (2) Snyder, C. E.; Gschwender, L. J.; Campbell, W. B. *Lubr. Eng.* **1982**, 38, 41.
- (3) Spool, A. M.; Kasai, P. H. *Macromolecules* **1996**, 29, 1691.
- (4) See for example, Willson, C. G. in *Introduction to Microlithography*; edited by Thompson, L. F.; Willson, C. G.; Bowden, M. J., American Chemistry Soc.: Washington, D. C. 1983; pp 122–140.
- (5) See, for example: Märk, T. D. in *Electron–Molecule Interactions and their Applications*; Christophorou, L. G., Ed.; Academic Press Inc.: London, 1984; pp 251–334.
- (6) Schueler, B.; Sander, P.; Reed, D. A. *Vacuum* **1990**, 41, 1661.
- (7) Schueler, B. *Microanal. Microstruct.* **1992**, 3, 1.
- (8) Briggs, D.; Hearn, M. J. *Vacuum* **1986**, 36, 1005.
- (9) Dewar, M. J. S.; Zoebisch, E. G.; Healy, E. F.; Stewart, J. P. *J. Am. Chem. Soc.* **1985**, 107, 3902. The program in HyperChem was used: *HyperChem* (Release 4); Hypercube, Inc.: Waterloo, Ontario, 1994.
- (10) Yanagisawa, M. *STLE Trib. Trans.* **1994**, SP-36, 25.
- (11) Hoinks, M.; Tober, E. D.; White, R. L.; Crowder, M. S. *Appl. Phys. Lett.* **1992**, 61, 2653.
- (12) Sohma, J. *Prog. Polym. Sci.* **1989**, 14, 451.